

Journal of Materials Science: Materials in Electronics

Intensification of iron-boron complex association in silicon solar cells under acoustic wave action --Manuscript Draft--

Manuscript Number:	JMSE-D-22-00483R1	
Full Title:	Intensification of iron-boron complex association in silicon solar cells under acoustic wave action	
Article Type:	Original Research	
Keywords:	Ultrasound; silicon solar cell; Iron-boron pair; Acousto-defect interaction	
Corresponding Author:	Oleg Olikh, Dr. hab. Taras Shevchenko National University of Kyiv: Kiivs'kij nacional'nij universitet imeni Tarasa Sevchenka Kyiv, UKRAINE	
Corresponding Author Secondary Information:		
Corresponding Author's Institution:	Taras Shevchenko National University of Kyiv: Kiivs'kij nacional'nij universitet imeni Tarasa Sevchenka	
Corresponding Author's Secondary Institution:		
First Author:	Oleg Olikh, Dr. hab.	
First Author Secondary Information:		
Order of Authors:	Oleg Olikh, Dr. hab.	
	Vitaliy Kostylyov, Dr.Sci.	
	Victor Vlasiuk, PhD	
	Roman Korkishko, PhD	
	Roman Chupryna	
Order of Authors Secondary Information:		
Funding Information:	National Research Foundation of Ukraine (2020.02/0036)	Not applicable
Abstract:	<p>In this paper, we study the influence of ultrasound (US) on the recovery of light-induced degradation in Cz-Si solar cells. The complete recovery in the dark at near room temperature and the determined value of activation energy (0.656 eV) evidenced the iron-boron pair transformation-related degradation. The ability of extraction of FeB pair's parameters from short circuit current kinetics was discussed.</p> <p>It was revealed that the US loading leads to the acceleration of the FeB pair association. This effect was investigated for different US frequencies (0.3-30 MHz) and intensities (up to 1.3 up to 1.3 W/cm²) as well as iron concentrations ((0.2-3)·10⁻¹³ cm⁻³) in the solar cell over temperature range 300-340 K. It has been found that US longitudinal waves are more efficient than transverse waves. The experimentally observed phenomena are related to the decrease in iron migration energy (up to 10 meV) in the US stress fields.</p>	
Additional Information:		
Question	Response	
Journal of Materials Science: Materials in Electronics considers only outstanding papers that make a distinct contribution to the field of experimental electronic materials. This includes optoelectronic	<p>Defect engineering is one of the most meaningful application tasks in semiconductors materials science.</p> <p>The irradiation and thermal treatment are ordinary ways to solve this problem. But the ultrasound showed abilities to affect defects as well.</p> <p>The manuscript focuses on the experimental investigation of the influence of acoustic</p>	

<p>and photonic materials as well.</p> <p>Please explain in point form why your work is outstanding and what distinguishes this work from past work. What are the outstanding and exceptional contributions of this paper? How does it contribute to the state-of-the art?</p>	<p>waves on iron, which is a critical impurity in silicon-based technology. The acoustically driven acceleration of the iron--boron complex association has been revealed.</p>
<p>Is this manuscript part of an ongoing Special Issue (SI), and were you asked to submit to this Special Issue?</p>	<p>No</p>
<p>Were you asked by one of our editors to resubmit your manuscript because of textual overlap or not complying with scientific guidelines?</p>	<p>No</p>

Dear Editor,

We like to express our appreciation to the reviewers for their comments. We are resubmitting the revised version of the paper number JMSE-D-22-00483. We have studied the comments of the reviewer carefully, and have changed the text according to the comments they have listed. The location of revisions is highlighted by yellow in “Marked-JMSE-D-22-00483.pdf”. Below we refer to each of the reviewer’s comments.

Response to Reviewer #1

Comment 1. *Since Ultrasound Stimulated (US) dissociation of FeB pairs in Silicon has been studied before, the author needs to give a short description of the work of reference 16 in the “Introduction” part.*

Reply: In fact, the possibility of the ultrasound to change the state of FeB was shown previously [1, 2]. In particular, the FeB pair was revealed [2] to be dissociated in Cz-Si by the action of ultrasound with acoustic strain $\xi_{US} = 10^{-5}$ – 10^{-4} . Furthermore, Ostapenko and Bell [2] regarded the resonance condition of pair dissociation and used 25–70 kHz. Besides, it was asserted [1] that in the case of predominant dissociated pairs, the ultrasound may promote the pairing reaction in contradistinction to the case of a high fraction of paired iron. But empirical evidence for this prediction is absent. In this work, i) the wave frequency $f_{US} = (0.3\text{--}30)$ MHz and subthreshold strain $\xi_{US} < 2 \times 10^{-6}$ were used, which were deficient overcome the Coulombic attraction between Fe_i^+ and B_s^- ; ii) the predominant dissociation of FeB was realized by intense illumination. Thus the association of FeB pair (the migration of Fe_i^+) was firstly investigated in conditions of USL.

The additional information was added to the revised manuscript (last paragraph in “Introduction”).

Comment 2. *The font in Figure 4 is obviously too small.*

Reply: The font was enlarged.

Comment 3. *The forms of the separation of axis titles and units are inconsistent in the Figures.*

Reply: All axis titles were changed according to “Axis title (unit)”.

Response to Reviewer #2

Comment 1. *Abstract: This part is precise and concise. It could be better to mention some points of the light induced degradation in solar cells.*

Reply: The different light-induced degradation (LID) phenomena exist that affect the efficiency of Cz-silicon solar cells due to a decrease in the lifetime of generated excess charge carriers. The main reasons for this transformation are boron–oxygen complex formation (BO-LID) [3] and iron–boron pair

dissociation (FeB-LID). Besides, the light- and elevated-temperature-induced degradation (LeTID) is observed. In recent studies, the occurrence of the LeTID defect is related to the presence of hydrogen and metal impurities [4–6]. We study the influence of ultrasound on LID recovery. The complete recovery in the dark at near room temperature and the determined value of activation energy (0.656 eV) evidenced the iron–boron pair LID in our case.

The text was revised (Abstract and page 4, paragraph 2).

Comment 2. *Introduction: Why not other doping elements ? why iron given more importance ? explanation required. Objective is not well framed.*

Reply: The silicon solar cells (SCs) constitute about 90% of current global photovoltaic production capacity. Iron is one of the most relevant, omnipresent, and efficiency-limiting metallic impurities in p-type silicon solar cells [7, 8]. Therefore, the methods of defect engineering aimed at iron have practical importance. On the one hand, shallow acceptors (B, Al, Ga, In) are effective trapping sites for iron around room temperature and in darkness in p-Si due to electrostatic attraction between the negatively charged acceptors and the positively charged iron ions. All Fe-acceptor pairs are similar: complexes have two structural configurations with trigonal and orthorhombic symmetry and can be broken by intense illumination and/or annealing above 200°C [7, 9]. On the other hand, the back surface field (BSF) cell and passivated emitter and rear cell (PERC) are the most popular designs that have been used in the mass-production of Si SCs, and both BSF and PERC are mainly based on boron-doped silicon wafers [10, 11]. Therefore the iron–boron pair is one of the most relevant complexes to the defect engineering in real SCs. The aim of this work is to investigate experimentally how acoustic waves (AWs) influence the ability of iron to diffuse in silicon SCs.

The text was revised (second and third paragraphs in “Introduction”).

Comment 3. *Experimental part: How much doping of phosphorus? How do they measure thickness?*

Reply: A diffusion from the gas phase (POCl_3) at 940°C was performed on wafers resulting in a n^+ -emitter layer on the front side (sheet resistance of about 20 – 30 Ω/\square , thickness of 0.7 μm). In addition, to reduce recombination losses and increase the conductivity of the contact layer, a p^+ layer (10 – 20 Ω/\square , 0.6 μm) was formed by boron diffusion from the gas phase (BCl_3) at 985°C on the rear surface. The solid and grid aluminum contacts were formed by magnetron sputtering on the rear and front surfaces, respectively.

The layer thicknesses were evaluated by using an annealing temperature and duration as well as an partial pressure gas.

More detailed information about samples was added (first paragraph in “Experimental and Calculation Details”).

Comment 4. *Why were AWs excited in the samples of 2.4; 4.1; 5.4; 9.0; 14; 18; 31 MHz (longitudinal) or 0.3 MHz (transverse) with frequency f_{US} ?. Give a reason. Why not selected substitution atoms?*

Reply: We have previously shown [12–17] that waves with megahertz frequency can be an effective tool for defect engineering in silicon structures. Thus in this work, we tried to use such waves to control iron impurities in silicon SCs.

On the other hand, it is widely known that the efficiency of ultrasound influence on defects in semiconductors depends on acoustic wave frequency. Moreover, the type of frequency dependence is determined by the mechanism of acousto-defect interaction [18–20]. The set of frequencies (2.4, 4.1, 5.4, 9.0, 14, 18, 31 MHz, longitudinal waves) was used to establish features of ultrasound influence on iron migration. Besides, the effect of the increase in the carrier capture coefficient for defects in silicon SC is shown [12] to be intensified in the case of the transverse acoustic waves using. Accordingly, the transverse waves (0.3 MHz) were used as well. In the case of acoustically-induced (AI) change of capture coefficient, the USL causes the variation in the complex components' distance [12]. In our case, the AI effect is the opposite and is weakened for transverse waves using. Therefore, the acceleration of the FeB pair association does not deal with iron-boron distance change.

The text was revised (second paragraph in “Experimental and Calculation Details”; page 8, paragraph 1).

Comment 5. *Result and discussion: In figure 5, x axis when will it reach minimum? Is there any particular reason for selecting 300 to 304K?*

Reply: The investigations have shown that the dependence of τ_{US}/τ_0 on ultrasound intensity is close to linear at low W_{US} . The increase in W_{US} leads to saturation, which correspond to $\tau_{US} \simeq 0.7\tau_0$ at $T = 340$ K. Therefore the minimum (saturation) of curves in Fig. 5 is expected at about 0.3 W/cm^2 . It should be noted that according to Ostapenko and Bell [2], the further increase in acoustic strain up to $\xi_{US} = 10^{-5}$ may lead to FeB pair dissociation and increase in τ_{US} .

The temperature range is limited for the following reasons. On the one hand, the investigations have shown that the ultrasound influence on FeB pair association time weakened with temperature decrease. In fact, the effect value is about 5% only for $T = 300$ K — see Fig. 6. Therefore the experiments seem useless at $T < 300$. On the other hand, the portion of interstitial iron atoms that remain unpaired in the equilibrium state increases with temperature rise. According to Wijaranakula [21], the concentration of unpaired iron atom $N_{Fei,eq}$ depends on temperature, doping level, and concentration of all iron impurity atoms $N_{Fe,0}$. The estimations show that at 340 K $N_{Fei,eq} \simeq 0.1N_{Fe,0}$. The further temperature decrease leads to an increase in $N_{Fei,eq}/N_{Fe,0}$ value and to a significant decrease in change of short circuit current after intense illumination and measurement accuracy of association time.

Response to Reviewer #3

Comment 1. *The results are new and may be considered for publication, however, the presentation of the contents is very poor and hence it is unacceptable in its present form. I guess, the main problem is with the English language used; many unconventional or unusual technical words, which make it difficult to understand what some descriptions mean.*

Reply: The text has been revised. We hope for the language improvement.

Comment 2. *1. Page 3, line 28, “Fig. 1 Scheme of the sample...” should be changed to, “Fig. 1 Schematic structure of the sample...”. And also in lines 33 -34, this should be changed as, “The schematic structure of SC...”.*

Reply: The Reviewer is absolutely right. We have revised the text accordingly.

Comment 3. *Fig. 2, presents the measured I_{sc} as a function of time of illumination t . Thus the y-axis of Fig. 2 should be labelled as I_{sc} (μA) and the x-axis as t (10^3 s). Also it is not explained what the red and green curves represent? The should explain Red with US and Green without US? Thus, the figure captions of Fig. 2 in lines 26-27 on page 4, should be changed to, “Measured I_{sc} plotted as a function of the illumination time t ; red curve- with US and green curve without US.”*

Reply: The figure captions was revised.

Comment 4. *3. The second paragraph, on page 4, lines 36-40, does not make any sense to me. It needs to be rewritten. It should emphasize how I_{sc} in Eq. (1) is obtained to represent the measure I_{sc} in Fig. 2.*

Reply: The FeB pair association in the dark was accompanied by the τ increase and was monitored by measuring the I_{SC} under LED illumination. The LED illumination induced excess carrier density $< 10^{12} \text{ cm}^{-3}$, had duty cycle 0.5% while $I_{SC}(t)$ measuring, and did not cause FeB dissociation. Moreover, the fitting of the measured dependencies $I_{SC}(t)$ after high-intensive illumination allows determining the pair concentration and the characteristic time of the FeB complex formation.

The text was revised. (page 5, paragraph 2).

Comment 5. *4. In Eq. (1) , please define all the symbols used. For example, what is P_{ph} ? Also if Eq. (1) represents the measured I_{sc} , why does it not depend on the time t ? This needs to be carefully explained.*

Reply: The Eq. (1) was modified, all symbols were defined. The parameters, which depend on time, were pointed in Eqs.(2),(3),(6) as well. In initial manuscript the P_{ph} (LED light power) was introduced on page 3, line 57.

Comment 6. Page 5, line 53, "... where τ_{ass} is the characteristic time of the complex association." This does not make sense to me. Do you mean, "... where τ_{ass} is the characteristic time of the formation of Fe-B complex ?" This needs to be fixed.

Reply: We have revised the text accordingly.

Comment 7. On page 6, lines 33-37, "... the values of $\tau_{ass} \dots 1380 \pm 20$ for $T = 330 \text{ K} \dots 1.26 \pm 0.02)10^4$ for $T = 300 \text{ K} \dots$ ". Something is wrong here? How can a 30 degree difference in temperature can give such a big value of τ_{ass} from Eq. (10).

Reply: According to [22–24]

$$\tau_{ass} = 5.7 \times 10^5 \frac{\text{s}}{\text{K cm}^3} \times \frac{T}{N_A} \exp\left(\frac{E_m}{kT}\right), \quad (1)$$

where E_m is the energy of Fe_i^+ migration, $E_m = 0.66 \text{ eV}$ [22–25]. Hence

$$\frac{\tau_{ass}(T = 300\text{K})}{\tau_{ass}(T = 330\text{K})} = \frac{300}{330} \times \exp\left[\frac{0.66}{8.625 \times 10^{-5}} \left(\frac{1}{300} - \frac{1}{330}\right)\right] \simeq 9.2. \quad (2)$$

At the same time

$$\frac{1.26 \times 10^4}{1380} \simeq 9.1. \quad (3)$$

$N_A = 1.4 \times 10^{15} \text{ cm}^{-3}$ for the samples under investigation. Therefore the experimentally determined times are close to ones expected from Eq. (1).

Comment 8. Page, 6 lines 53-57, the first sentence of Results and Discussion does not make any sense. Please rewrite it.

Reply: The sentence was rewrite in form "The experiments have shown that the US loading leads to speed up of recovery of short circuit current after high-intensive illumination. Therefore, the FeB association is intensified under AW action."

Comment 9. Page 6, lines 60-61, "The figure also shows τ_{ass} values..." but figure 3 does not show any τ_{ass} ? Please check it and fix it carefully.

Reply: Figure 3 presents the measured short circuit current (marks), the fitting curves (lines), and the pair formation time constants determined by the

fitting (labels). The text (first paragraph in “Results and Discussion”) was revised.

References

- [1] Ostapenko, S.S., Jastrzebski, L., Lagowski, J., Sopori, B.: Increasing short minority carrier diffusion lengths in solar-grade polycrystalline silicon by ultrasound treatment. *Appl. Phys. Lett.* **65**(12), 1555–1557 (1994). <https://doi.org/10.1063/1.112942>
- [2] Ostapenko, S.S., Bell, R.E.: Ultrasound stimulated dissociation of Fe–B pairs in silicon. *J. Appl. Phys.* **77**(10), 5458–5460 (1995). <https://doi.org/10.1063/1.359243>
- [3] Lindroos, J., Savin, H.: Review of light-induced degradation in crystalline silicon solar cells. *Sol. Energy Mater. Sol. Cells* **147**, 115–126 (2016). <https://doi.org/10.1016/j.solmat.2015.11.047>
- [4] Schmid, A., Fischer, C., Skorka, D., Herguth, A., Winter, C., Zuschlag, A., Hahn, G.: On the role of AlO_x thickness in AlO_x/SiN_y: H layer stacks regarding light- and elevated temperature-induced degradation and hydrogen diffusion in c-Si. *IEEE Journal of Photovoltaics* **11**(4), 967–973 (2021). <https://doi.org/10.1109/JPHOTOV.2021.3075850>
- [5] Wagner, M., Wolny, F., Hentsche, M., Krause, A., Sylla, L., Kropfgans, F., Ernst, M., Zierer, R., Bönisch, P., Müller, P., Schmidt, N., Osinniy, V., Hartmann, H.-P., Mehnert, R., Neuhaus, H.: Correlation of the LeTID amplitude to the Aluminium bulk concentration and Oxygen precipitation in PERC solar cells. *Sol. Energy Mater. Sol. Cells* **187**, 176–188 (2018). <https://doi.org/10.1016/j.solmat.2018.06.009>
- [6] Chen, D., Kim, M., Stefani, B.V., Hallam, B.J., Abbott, M.D., Chan, C.E., Chen, R., Payne, D.N.R., Nampalli, N., Ciesla, A., Fung, T.H., Kim, K., Wenham, S.R.: Evidence of an identical firing-activated carrier-induced defect in monocrystalline and multicrystalline silicon. *Sol. Energy Mater. Sol. Cells* **172**, 293–300 (2017). <https://doi.org/10.1016/j.solmat.2017.08.003>
- [7] Istratov, A.A., Hieslmair, H., Weber, E.R.: Iron and its complexes in silicon. *Applied Physics A: Materials Science & Processing* **69**(1), 13–44 (1999). <https://doi.org/10.1007/s003390050968>
- [8] Schubert, M.C., Padilla, M., Michl, B., Mundt, L., Giesecke, J., Hohl-Ebinger, J., Benick, J., Warta, W., Tajima, M., Ogura, A.: Iron related solar cell instability: Imaging analysis and impact on cell performance. *Sol. Energy Mater. Sol. Cells* **138**, 96–101 (2015). <https://doi.org/10.1016/j.solmat.2015.03.001>

- [9] Bartel, T., Gibaja, F., Graf, O., Gross, D., Kaes, M., Heuer, M., Kirscht, F., Möller, C., Lauer, K.: Dynamics of iron-acceptor-pair formation in co-doped silicon. *Appl. Phys. Lett.* **103**(20), 202109 (2013). <https://doi.org/10.1063/1.4830227>
- [10] Ajayan, J., Nirmal, D., Mohankumar, P., Saravanan, M., Jagadesh, M., Arivazhagan, L.: A review of photovoltaic performance of organic/inorganic solar cells for future renewable and sustainable energy technologies. *Superlattices Microstruct.* **143**, 106549 (2020). <https://doi.org/10.1016/j.spmi.2020.106549>
- [11] Green, M.A.: Photovoltaic technology and visions for the future. *Prog. Energy* **1**(1), 013001 (2019). <https://doi.org/10.1088/2516-1083/ab0fa8>
- [12] Olikh, O.Y.: Acoustically driven degradation in single crystalline silicon solar cell. *Superlattices Microstruct.* **117**, 173–188 (2018). <https://doi.org/10.1016/j.spmi.2018.03.027>
- [13] Olikh, O.Y., Gorb, A.M., Chupryna, R.G., Pristay–Fenenkov, O.V.: Acousto–defect interaction in irradiated and non–irradiated silicon n^+p structure. *J. Appl. Phys.* **123**(16), 161573 (2018). <https://doi.org/10.1063/1.5001123>
- [14] Olikh, O.Y., Voytenko, K.V., Burbelo, R.M.: Ultrasound influence on I–V–T characteristics of silicon Schottky barrier structure. *J. Appl. Phys.* **117**(4), 044505 (2015). <https://doi.org/10.1063/1.4906844>
- [15] Gorb, A.M., Korotchenkov, O.A., Olikh, O.Y., Podolian, A.O., Chupryna, R.G.: Influence of γ –irradiation and ultrasound treatment on current mechanism in au-sio₂-si structure. *Solid-State Electron.* **165**, 107712 (2020). <https://doi.org/10.1016/j.sse.2019.107712>
- [16] Olikh, O.: Reversible influence of ultrasound on γ –irradiated Mo/n-Si Schottky barrier structure. *Ultrasonics* **56**, 545–550 (2015). <https://doi.org/10.1016/j.ultras.2014.10.008>
- [17] Olikh, O., Voytenko, K.: On the mechanism of ultrasonic loading effect in silicon–based Schottky diodes. *Ultrasonics* **66**(1), 1–3 (2016). <https://doi.org/10.1016/j.ultras.2015.12.001>
- [18] Brailsford, A.D.: Abrupt–kink model of dislocation motion. *Phys. Rev.* **122**(3), 778–786 (1961). <https://doi.org/10.1103/PhysRev.122.778>
- [19] Pavlovich, V.N.: Enhanced diffusion of impurities and defects in crystals in conditions of ultrasonic and radiative excitation of the crystal lattice. *Phys. Status Solidi B* **180**(1), 97–105 (1993). <https://doi.org/10.1002/pssb.2221800108>

- [20] Peleshchak, R.M., Kuzyk, O.V., Dan'kiv, O.O.: Formation of periodic structures under the influence of an acoustic wave in semiconductors with a two-component defect subsystem. *Ukr. J. Phys.* **61**(8), 741–746 (2016). <https://doi.org/10.15407/ujpe61.08.0741>
- [21] Wijaranakula, W.: The reaction kinetics of iron–boron pair formation and dissociation in p-type silicon. *J. Electrochem. Soc.* **140**(1), 275–281 (1993). <https://doi.org/10.1149/1.2056102>
- [22] Khelifati, N., Laine, H.S., Vähänissi, V., Savin, H., Bouamama, F.Z., Bouhafs, D.: Dissociation and formation kinetics of iron–boron pairs in silicon after phosphorus implantation gettering. *Phys Status Solidi A* **216**(17), 1900253 (2019). <https://doi.org/10.1002/pssa.201900253>
- [23] Möller, C., Bartel, T., Gibaja, F., Lauer, K.: Iron-boron pairing kinetics in illuminated p-type and in boron/phosphorus co-doped n-type silicon. *J. Appl. Phys.* **116**(2), 024503 (2014). <https://doi.org/10.1063/1.4889817>
- [24] Tan, J., Macdonald, D., Rougieux, F., Cuevas, A.: Accurate measurement of the formation rate of iron–boron pairs in silicon. *Semicond Sci. Technol.* **26**(5), 055019 (2011). <https://doi.org/10.1088/0268-1242/26/5/055019>
- [25] Macdonald, D., Cuevas, A., Geerligs, L.J.: Measuring dopant concentrations in compensated p-type crystalline silicon via iron–acceptor pairing. *Appl. Phys. Lett.* **92**(20), 202119 (2008). <https://doi.org/10.1063/1.2936840>

Intensification of iron-boron complex
association in silicon solar cells under
acoustic wave action

Oleg Olikh^{1*}, Vitaliy Kostylyov², Victor Vlasiuk², Roman
Korkishko² and Roman Chupryna¹

¹Physics faculty, Taras Shevchenko National University of Kyiv,
64/13, Volodymyrska Street, Kyiv, 01601, Ukraine.

²V. Lashkaryov Institute of Semiconductor Physic of NAS of
Ukraine, 41, pr. Nauki, Kyiv, 03028, Ukraine.

*Corresponding author(s). E-mail(s): olegolikh@knu.ua;
Contributing authors: vkost@isp.kiev.ua;
viktorvlasiuk@gmail.com; romkin.ua@gmail.com;
r_chupryna@voliacable.com;

Abstract

In this paper, we study the influence of ultrasound (US) on the recovery of light-induced degradation in Cz-Si solar cells. The complete recovery in the dark at near room temperature and the determined value of activation energy (0.656 eV) evidenced the iron–boron pair transformation-related degradation. The ability of extraction of FeB pair’s parameters from short circuit current kinetics was discussed. It was revealed that the US loading leads to the acceleration of the FeB pair association. This effect was investigated for different US frequencies (0.3–30 MHz) and intensities (up to 1.3 W/cm²) as well as iron concentrations ((0.2–3)×10¹³ cm^{−3}) in the solar cell over temperature range 300–340 K. It has been found that US longitudinal waves are more efficient than transverse waves. The experimentally observed phenomena are related to the decrease in iron migration energy (up to 10 meV) in the US stress fields.

Keywords: Ultrasound, Silicon solar cell, Iron-boron pair, Acousto-defect interaction

1 Introduction

It is well known that ultrasound (US) can act efficiently on defect subsystems of semiconductor crystals and devices due to dissipation of US vibration energy, which is particularly intense in regions with periodicity disorder [1–3]. At US of subthreshold intensity, acoustically induced (AI) reconstruction of defects causes the reversible changes in charge concentration and mobility in crystals [4, 5], barrier height in Schottky structures [6, 7] as well as tunnel and recombination currents in p-n structures [3, 8]. Also, it seems promising to apply the US as an additional factor of influence during conventional technological processes. In this case, semiconductor structures are usually found in nonequilibrium conditions, and the defect–impurity subsystem is capable of modifying easier under the action of elastic oscillations. For instance, the application of ultrasound loading (USL) during ion implantation facilitates the formation of ultra-shallow junctions [9], and intensifies the silicon surface layer amorphization [10]; USL applied during the production of porous silicon results in structural ordering [11] and when applied during ZnO deposition provides higher homogeneity of the films [12].

The silicon solar cells (SCs) constitute about 90% of the global photovoltaic production capacity. Iron is one of the most relevant, omnipresent, and efficiency-limiting metallic impurities in p-type Si SCs [13, 14]. Therefore, the methods of defect engineering aimed at iron have practical importance. In silicon photovoltaics, one of the main methods of impurity deactivation and removing it from the operation zone is gettering Fe atoms at certain centers (extended defects, oxygen precipitates, or interfaces) [15]. A similar gettering can be realized during standard operations as phosphorus diffusion [16] or production of antireflection coating [17]. It is clear that the process efficiency depends on the mobility of iron atoms.

On the one hand, shallow acceptors (B, Al, Ga, In) are effective trapping sites for iron around room temperature and in darkness in p-Si due to electrostatic attraction between the negatively charged acceptors and the positively charged iron ions. All Fe-acceptor pairs are similar: complexes have two structural configurations with trigonal and orthorhombic symmetry and can be broken by intense illumination and/or annealing above 200°C [13, 18]. On the other hand, the back surface field (BSF) cell and passivated emitter and rear cell (PERC) are the most popular designs that have been used in the mass-production of Si SCs, and both BSF and PERC are mainly based on boron-doped silicon wafers [19, 20]. Therefore the iron–boron pair is one of the most relevant complexes to the defect engineering in real SCs. This work aims to investigate experimentally how acoustic waves (AWs) influence the ability of iron to diffuse in silicon solar cells. The time of iron–boron pair association after light-induced dissociation was used as an indicator of iron ion mobility. The possibility of the ultrasound to change the state of FeB was shown previously [21, 22]. In particular, the FeB pair was revealed [22] to be dissociated in Cz-Si by the action of ultrasound with acoustic strain $\xi_{\text{US}} = 10^{-5}$ – 10^{-4} . Furthermore, Ostapenko and Bell [22] regarded the resonance condition of

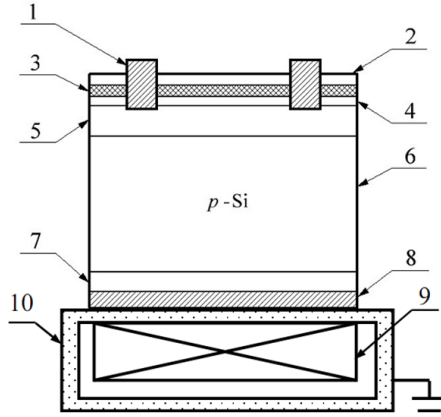


Fig. 1 Schematic structure of the sample and USL. 1 — frontal grid electrode (Al); 2 — Si_3N_4 (40 nm); 3 — SiO_2 (30 nm); 4 — induced n^{++} -layer; 5 — diffusion n^+ -layer; 6 — quasineutral base region of p -type (350 μm); 7 — diffusion p^+ -layer; 8 — rear metallization (Al); 9 — piezoelectric transducer; 10 — metal foil (Cu)

pair dissociation and used 25–70 kHz. Besides, it was asserted [21] that in the case of predominant dissociated pairs, the ultrasound may promote the pairing reaction in contradistinction to the case of a high fraction of paired iron. But empirical evidence for this prediction is absent. In this work, i) the wave frequency $f_{\text{US}} = (0.3\text{--}30)$ MHz and subthreshold strain $\xi_{\text{US}} < 2 \times 10^{-6}$ were used, which were deficient overcome the Coulombic attraction between Fe_i and B_s^- ; ii) the predominant dissociation of FeB was realized by intense illumination. Thus the association of FeB pair (the migration of Fe_i^+) was firstly investigated in conditions of USL.

2 Experimental and Calculation Details

Experimental studies were performed on the samples of silicon SC ($1.52 \times 1.535 \text{ cm}^2$) made based on single-crystal p -type silicon [100] wafers with the resistivity of about 10 $\Omega\cdot\text{cm}$ (boron doping level $N_A = 1.4 \times 10^{15} \text{ cm}^{-3}$). The thickness of the wafers was 380 μm . Diffusion from the gas phase (POCl_3) at 940°C was performed on wafers resulting in an n^+ -emitter layer on the front side (sheet resistance of about 20 – 30 Ω/\square , thickness of 0.7 μm). In addition, to reduce recombination losses and increase the conductivity of the contact layer, a p^+ layer (10 – 20 Ω/\square , 0.6 μm) was formed by boron diffusion from the gas phase (BCl_3) at 985°C on the rear surface. Layers of SiO_2 and Si_3N_4 were formed on the front surface of the SC to passivate the surface and reduce the optical reflectance. The solid and grid aluminum contacts were formed by magnetron sputtering on the rear and front surfaces, respectively. The schematic structure of SC is presented in Fig. 1.

In the case of USL, the transverse or longitudinal AWs were applied to the samples in [100] direction by using LiNbO_3 or ceramic piezoelectric transducer.

4 *Intensification of FeB association in Si-SCs by acoustic wave*

The transducer was attached to the whole area of Al back contact. It is widely known that the efficiency of ultrasound influence on defects in semiconductors depends on acoustic wave frequency f_{US} . Moreover, the type of frequency dependence is determined by the mechanism of acousto-defect interaction [23–25]. The set of frequencies (2.4, 4.1, 5.4, 9.0, 14, 18, and 31 MHz, longitudinal waves) was used to establish features of ultrasound influence on iron migration. Besides, the effect of the increase in the carrier capture coefficient for defects in silicon SC is shown [26] to be intensified in the case of the transverse acoustic waves using. Accordingly, the transverse waves ($f_{\text{US}} = 0.3$ MHz) were used as well. The ultrasound intensities W_{US} did not overcome 1.3 W/cm^2 . To avoid the effect of the piezoelectric field on the measurements procedure as well as sample parameters, the transducer was shielded by Cu foil — see Fig. 1.

It is known that Fe in silicon can be in two states: in the form of FeB pair or in the interstitial state Fe_i . At near room temperature and boron concentration $> 10^{14} \text{ cm}^{-3}$, almost all Fe bound in FeB pairs is in equilibrium [27–30]. However, numerous researches show that dissociation of pairs can be performed either by heating to the temperature above 200°C or by intense illumination at room temperature [28, 30]. In our work, we used the latter approach, and the high-intensive illumination source was a halogen lamp with a radiation intensity of about 250 mW/cm^2 . To dissociate FeB pairs, the front side of the sample was illuminated, and the illumination time was 30 s.

The different light-induced degradation (LID) phenomena exist that affect the efficiency of Cz-silicon solar cells due to a decrease in the lifetime of generated excess charge carriers. The main reasons for this transformation are boron–oxygen complex formation (BO-LID) [31] and iron–boron pair dissociation. Besides, the light- and elevated-temperature-induced degradation (LeTID) is observed. In recent studies, the occurrence of the LeTID defect is related to the presence of hydrogen and metal impurities [32–34]. The complete recovery in the dark at near room temperature and the determined value of activation energy (0.656 eV, see below) evidenced the iron–boron pair-related LID in our case.

It is known that FeB pair dissociations in the SC base are accompanied by the change in the lifetime of minority carriers τ . As an indicator of τ , we considered short circuit current I_{SC} , which was measured under SC illumination by a low-intensive monochromatic light. The low-intensive source was a light-emitting diode (LED) with radiation power $P_{\text{ph}} \sim 350 \text{ }\mu\text{W}$ (measured by PowerMeter Rk-5720) and wavelength $\lambda = 940 \text{ nm}$.

The kinetics of short circuit current was measured after high-intensive illumination (see Fig. 2). The measurements were carried out over a temperature range of 300–340 K. The temperature was varied by a thermoelectric cooler and stabilized by a computer-controlled PID loop to better than 0.05 K. The temperature was controlled by STS-21 sensor, which was placed on the front surface of SC.

The FeB pair association in the dark was accompanied by the τ increase and was monitored by measuring the I_{SC} under LED illumination with 940

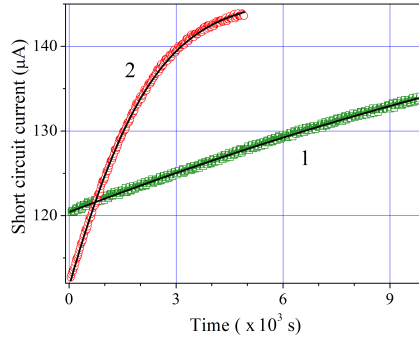


Fig. 2 Measured under low-intensive (LED) illumination short circuit current plotted as a function of the time after high-intensive (halogen lamp) illumination. The marks are the experimental results, the lines are the fitted curves using Eqs. (1)-(9). The zero of time corresponds to the moment of intensive illumination termination. T , K: 300 (1, green squares), 330 (2, red circles)

nm wavelength. The LED illumination induced excess carrier density $\Delta n < 10^{12} \text{ cm}^{-3}$, had duty cycle 0.5% while $I_{SC}(t)$ measuring, and did not cause FeB dissociation. Moreover, the fitting of the measured dependencies $I_{SC}(t)$ after high-intensive illumination allows determining the pair concentration and the characteristic time of the FeB complex formation. In fact, in conditions of homogeneous carrier generation in the base by the LED illumination, the short circuit current can be described as follows [35, 36]:

$$I_{SC}(t) = \frac{P_{ph}(1 - R_{ph})q\beta\lambda}{hc} \frac{\alpha_{ph}L_n(t)}{1 + \alpha_{ph}L_n(t)}, \quad (1)$$

where P_{ph} is the LED light power, λ is the light wavelength (940 nm), q is elementary charge, h is the Planck constant, c is the speed of light, $\alpha_{ph} = \alpha_{ph}(T)$ is the coefficient of light absorption, which was calculated according to [37, 38], T is the cell temperature, $R_{ph}(\lambda)$ is the coefficient of reflection, which was calculated for used samples according to [39, 40], $R_{ph}(940 \text{ nm}) = 0.14$; β is the coefficient of quantum yield, $\beta = 1$; L_n is the diffusion length of minority carriers. In its turn

$$L_n(t) = \sqrt{\frac{\mu_n k T \tau(t)}{q}}, \quad (2)$$

where μ_n is the electron mobility, was calculated by Klaassen theory [41], k is the Boltzmann constant.

In the assumption that it is the iron-related defects that play an essential role in the recombination, the following expression can be used to estimate τ according to Mattisen rule:

$$\tau(t)^{-1} = \tau_{rad}^{-1} + \tau_{Aug}^{-1} + (\tau_{SRH}^{Fe_i}(t))^{-1} + (\tau_{SRH}^{FeB}(t))^{-1} + \tau_{other}^{-1}, \quad (3)$$

6 *Intensification of FeB association in Si-SCs by acoustic wave*

where τ_{rad} and τ_{Aug} are associated with band-to-band radiation recombination and Auger processes, respectively; $\tau_{SRH}^{Fe_i}$ and τ_{SRH}^{FeB} are related to the recombinations at interstitial iron atoms Fe_i and at FeB pairs, accordingly; τ_{other} describes further recombination channels including surface recombination. In turn,

$$\tau_{rad}^{-1} = B(N_A + n_0 + \Delta n), \quad (4)$$

$$\tau_{Aug}^{-1} = C_p N_A^2, \quad (5)$$

where the values of recombination coefficients B and C_p were calculated by data from [42, 43]; $n_0 = n_i^2/N_A$ and intrinsic carrier concentration n_i was taken from [44].

In order to calculate $\tau_{SRH}^{Fe_i}$ and τ_{SRH}^{FeB} , Shockley–Read–Hall model was used:

$$\tau_{SRH}^{Fe_i, FeB}(t) = \frac{\tau_{p0}(t)(n_0 + n_1 + \Delta n) + \tau_{n0}(t)(N_A + p_1 + \Delta n)}{N_A + n_0 + \Delta n}, \quad (6)$$

where $\tau_{p0,n0}(t) = (N_{trap}(t)\sigma_{p,n}v_{th}^{p,n})^{-1}$, $N_{trap}(t)$ is the trap concentration (N_{Fe_i} and N_{FeB} for Fe_i and FeB, respectively), σ_n , σ_p are the cross sections of the recombination centers for electrons and holes, respectively, v_{th}^n , v_{th}^p are the average thermal velocities of electrons and holes calculated according to [45], $n_1 = N_C \exp(-(E_C - E_t)/kT)$, $p_1 = N_V \exp(-(E_t - E_V)/kT)$; N_C and N_V are the densities of states in the conduction band and valence band, respectively [44]; E_C and E_V are the energy of the conduction band and valence band edge, respectively; E_t is the energy level of the relevant recombination level. The parameters of recombination centers related to Fe_i and FeB were taken from [46].

The time dependence of interstitial iron atom concentration after pair dissociations is described by the known expression from [47]:

$$N_{Fe_i}(t) = (N_{Fe_i,0} - N_{Fe_i,eq}) \cdot \exp(-t/\tau_{ass}) + N_{Fe_i,eq}, \quad (7)$$

where τ_{ass} is the characteristic time of the formation of FeB pair, $N_{Fe_i,0}$ is the concentration of interstitial iron atoms formed due to high-intensive illumination, $N_{Fe_i,eq}$ is the part of interstitial iron atoms with $N_{Fe_i,0}$ that remain unpaired in equilibrium state (after a long exposition in darkness)[27]:

$$N_{Fe_i,eq} = \frac{N_{Fe_i,0}}{\left[1 + N_A 10^{-23} \exp\left(\frac{0.582\text{eV}}{kT}\right)\right] \left[1 + \exp\left(-\frac{E_F - 0.394\text{eV}}{kT}\right)\right]}, \quad (8)$$

E_F is the quasi-Fermi level.

In its turn, the iron–boron pair concentration N_{FeB} , which formed as the result of the partial association of $N_{Fe_i,0}$, should be described by the following expression:

$$N_{FeB}(t) = N_{Fe_i,0} - N_{Fe_i}(t). \quad (9)$$

We used Eqs. (1)–(9) to fit the measured time dependencies of short circuit current — see the examples in Fig. 2. The fitting was performed by using meta-heuristic method EBLSHADE [48]; as fitting parameters, P_{ph} , τ_{other} , $N_{Fe_i,0}$,

and τ_{ass} were taken. Thus, for the experimental data given in Fig. 2, the following parameter values were determined. $P_{ph} = (3.2 \pm 0.3) \times 10^{-4}$ W, which agrees well with the measured by PowerMeter Rk-5720 value ($350 \mu\text{W}$). $\tau_{other} > 100$ s, which testifies that the other recombination channel (other impurities, lattice defects, surface recombination) can be neglected. $N_{\text{Fe}_i,0} = (7 \pm 1) \times 10^{12} \text{ cm}^{-3}$, which is, on the one hand, a typical value for solar silicon, and, on the other hand, it is close to $3 \times 10^{12} \text{ cm}^{-3}$ obtained for the samples of the same series from L_n measuring before and after high-intense illumination [49]. Finally, the values of τ_{ass} were found to be (1380 ± 20) s at $T = 330$ K and $(1.26 \pm 0.02) \times 10^4$ s at $T = 300$ K. It was reported that τ_{ass} depends on the boron concentration and temperature, and the following expression was proposed for association characteristic time [28]:

$$\tau_{ass} = \frac{5.7 \times 10^5 T}{N_A} \exp\left(\frac{E_m}{kT}\right), \quad (10)$$

where E_m is the energy of Fe_i migration.

The value $E_m = (0.656 \pm 0.002)$ eV was calculated by using Eq. (10) and τ_{ass} , which determined from experiment. This value coincides with the well-known [28, 50] value of 0.66 eV. The coincidence proves that the measuring of the time dependence of short circuit current after high-intensive illumination can be applied in finding such parameters of iron-related defects as FeB pair association time and Fe concentration.

3 Results and Discussion

The typical dependencies $I_{SC}(t)$, measured at different temperatures under USL conditions and without USL, are given in Fig. 3. The experiments have shown that the US loading leads to a speed-up of recovery of short circuit current after high-intensive illumination. Therefore, the FeB association is intensified under AW action. The pair formation time constant, determined by the measured data fitting in the case of ultrasound loading, will be referred to as τ_{US} ($\tau_{US} = \tau_{ass}@W_{US} > 0$). In its turn, the time constant, determined in the case without ultrasound, will be referred to as τ_0 ($\tau_0 = \tau_{ass}@W_{US} = 0$). τ_{US} and τ_0 are given in Fig. 3 as well. As seen, $\tau_{US}/\tau_0 < 1$. To evaluate the acoustically induced accelerating of FeB pair formation, the τ_{US}/τ_0 magnitude will be used hereafter.

The obtained results show that the magnitude of speed-up of FeB pair formation depends on AW intensity. As shown in Fig. 4, the τ_{US} decreases with the increase in ultrasound intensity, and the dependence of τ_{US} on W_{US} is close to linear at low values of intensity. The increase in W_{US} leads to the τ_{US} saturation. In the saturation case, τ_{US} equals to about $0.7\tau_0$ at 340 K.

Also, Fig. 4 shows that the efficiency of AI accelerating of FeB pair formation decreases with the increase in US frequency. This feature is observed for the samples with different iron content. The iron concentrations were determined by fitting of $I_{SC}(t)$ dependencies, which were measured at complete FeB

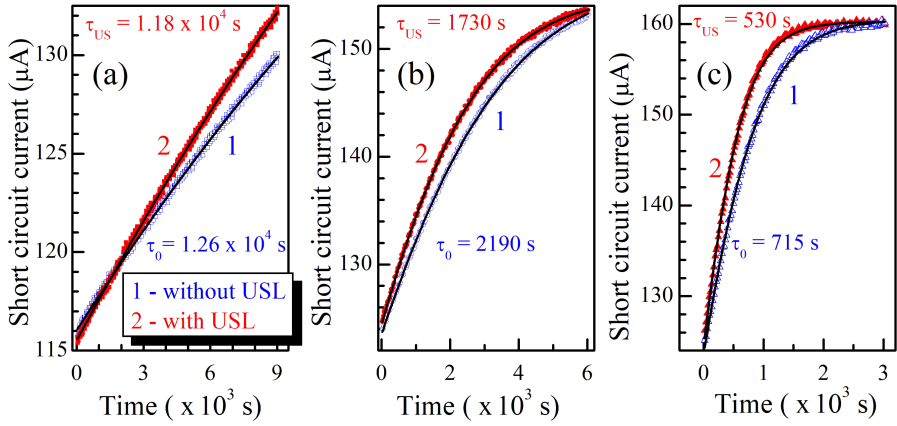


Fig. 3 Measured short circuit current plotted as a function of the time after high-intensive illumination under USL (1, filled red marks, $f_{US} = 2.4$ MHz) and without USL (2, empty blue marks). The lines are the fitted curves using Eqs. (1)-(9). T , K: 300 (a), 320 (b), 340 (c). The pair formation time constants determined by the fitting are shown as well; τ_{US} (red) — with USL and τ_0 (blue) — without USL

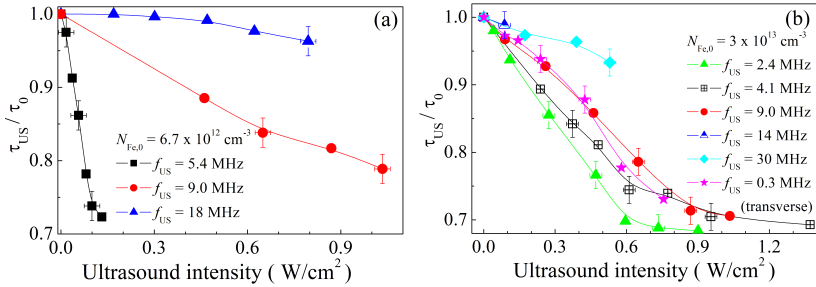


Fig. 4 The dependencies of AI accelerating of FeB pair formation on the US intensity at different f_{US} . Parts a and b present results for the Si solar cells with different iron concentrations. $T = 340$ K. The marks are the experimental results, the lines are given for convenience only

pairs dissociation conditions (i.e., in the case of high-intensive illumination with duration ≥ 30 s, which cause a maximum decrease in short circuit current value). The US intensity $W_{US,sat}$, which corresponds to saturation in τ_{US}/τ_0 , depends on f_{US} as well: in fact, $W_{US,sat} \simeq 0.6$ W/cm² at $f_{US} = 2.4$ MHz and $W_{US,sat} \simeq 0.9$ W/cm² at $f_{US} = 9.0$ MHz — see Fig. 4(b). At the same time, the saturation magnitude of τ_{US}/τ_0 does not depend on f_{US} . Transverse waves, despite lower frequency, affect the processes of FeB pair formation more weakly. It is previously shown [26] that the acoustically-induced change of complex defect parameters can be attributed to the variation in the distance of the components, and this effect is intensified in the case of the transverse waves. The opposite feature of investigated phenomenon testifies that the AI

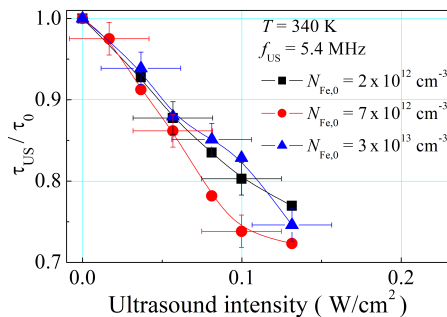


Fig. 5 The dependencies of AI accelerating of FeB pair formation on the US intensity in solar cells with different iron content. $T = 340$ K. $f_{US} = 5.4$ MHz. The marks are the experimental results, the lines are given for convenience only

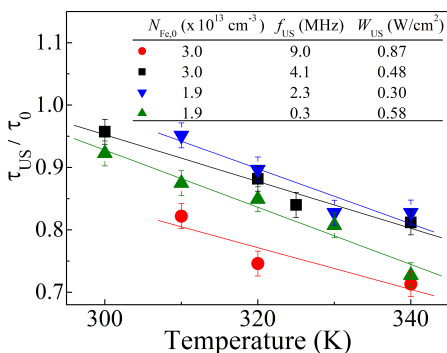


Fig. 6 Temperature dependencies of AI accelerating of FeB pair formation. The marks are the experimental results, the lines are the linear fitted curves

acceleration of the FeB pair association does not deal with change in the iron-boron distance. The following figure, Fig. 5, presents τ_{US}/τ_0 dependencies for the samples with different iron concentrations under USL of the same US frequency. As seen from the figure, the AI effect does not practically depend on $N_{Fe,0}$.

Figure 6 illustrates the variation of US impact on the characteristic FeB pair association time over the explored temperature range. The data for $f_{US} = 9.0$ MHz is correspond to the saturation region of $\tau_{US}/\tau_0 = f(W_{US})$ dependency, other data — to the linear region. As seen from the figure, the temperature decrease causes the decrease in efficiency of US influence, and the dependencies of τ_{US}/τ_0 on T are close to linear.

The association of the FeB complex happens at the expense of Fe_i diffusion towards the boron atoms located in substituting positions and strongly bound with the neighbor due to forming covalent bonds with them. Therefore, the τ_{ass} depends on the coefficient of iron diffusion D_{Fe} , so a more detailed, in

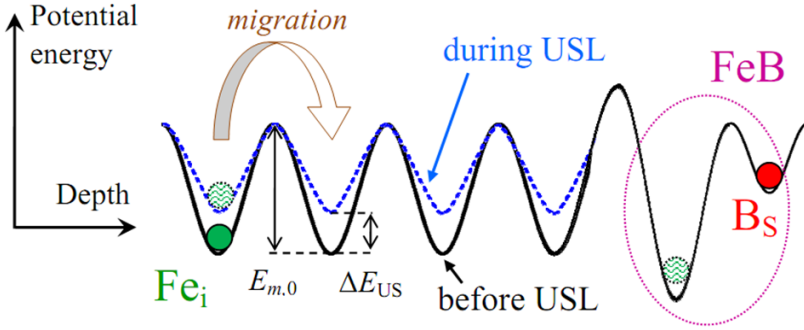


Fig. 7 A schematic picture showing the spatial variation of the potential energy of iron interstitial atom in Si as a function of position near the boron substitutional atom. US stress lowers the energy barrier for Fe migration. The curves are scaled arbitrarily

comparison with Eq. (10), the expression takes the following form [28, 30, 51]:

$$\tau_{ass} = \frac{\varepsilon \varepsilon_0 kT}{q^2 D_{Fe} N_A} = \frac{\varepsilon \varepsilon_0 kT}{q^2 D_{0,Fe} N_A} \exp\left(\frac{E_m}{kT}\right), \quad (11)$$

where ε is the dielectric constant of silicon, ε_0 is the vacuum permittivity, $D_{Fe} = D_{0,Fe} \exp(-E_m/kT)$, $D_{0,Fe}$ is the temperature-independent multiplier, in the general case [52–54] $D_{0,Fe} = \beta \nu a^2 \exp(\delta S_{Fe}/k)$, β is the correlation factor, ν is the effective vibrational (attempt) frequency, a is the jump distance, δS_{Fe} is the migration entropy.

As seen from the Eq. (11), the decrease FeB pair formation time under USL condition testifies about AI increase in D_{Fe} . In our opinion, the most probable reason is AI decrease in iron migration energy — see Fig. 7. Enhanced diffusion of impurities in the US field was observed previously in poly- and single-crystals of silicon and gallium arsenide [55, 56]. The decrease in interstitial iron atom migration energy can be given as

$$E_m \xrightarrow{\text{ultrasound}} E_{m,0} - \Delta E_{US}, \quad (12)$$

where $E_{m,0}$ is the migration energy without USL, according to [28, 50] and our estimation, $E_{m,0} \sim 0.66$ eV; ΔE_{US} is the AI change in migration energy. According to the obtained results, energy change depends on temperature and US characteristics ($\Delta E_{US} = f(W_{US}, f_{US}, \text{wavetype}, T)$) and does not exceed 10 meV.

The mechanism of the found AI phenomenon can be the following. By using thermodynamic formalism, it was shown [52] that the ability of impurities in Si to diffuse depends on mechanical stress η :

$$\frac{D(\eta)}{D(0)} = \exp\left(\frac{\eta V^*}{kT}\right) = \exp\left(\frac{\eta[-\Omega + V^r + V^m]}{kT}\right), \quad (13)$$

where V^* is the activation strain tensor, Ω is the atomic volume representing crystal dimension changes upon the formation of lattice site before the lattice

relaxation around the newly created point defect is permitted, V^r is the relaxation volume, V^m is the migration strain tensor, which characterizes stress impact on the defect mobility. The enhance Fe_i diffusivity in the strain field is discussed in [57] as well.

In our opinion, this reason explains the found US impact on FeB pairs formation in silicon solar cell. In fact, as seen from the Eq. (13), the stress-induced change in diffusion coefficient is thermally activated. As a result, the AI variation in τ_{ass} depends on temperature. In addition, generally V^* contains 81 components [52]; therefore change in D_{Fe} depends on the direction of atom elastic displacements. This accounts for the less effective impact of transverse waves. It should be noted, that the absorption of oscillation energy is used [58, 59] to reveal the cause of USL impact on defect system in Si-SiO₂ structures, and, in particular, AI increase in impurities mobility.

The results reported here open up new possibilities in manipulating electronic properties of silicon barrier devices. For example, as mentioned above, during phosphor diffusion, the iron impurity gettering occurs as well. The diffusion happens at high temperatures, and iron is in an unpaired interstitial state. USL applied during this technological process should increase the degree of the SC base region cleaning due to AI increase in Fe diffusion coefficient and, as a result, improve SC performance.

4 Conclusion

The ultrasound influence on FeB pair formation in silicon solar cells has been investigated experimentally. The investigation has revealed an acoustically driven decrease in the association characteristic time, which was caused by enhancing in iron atom diffusivity under ultrasound action. The effect is intensified with the increase in temperature and the decrease in ultrasound frequency. The application of longitudinal acoustic waves is more effective than transverse waves. The phenomenon can be related to reducing iron migration energy (up to 10 meV) in silicon under ultrasound stress at nearly-room temperature. Thus, ultrasound can be an effective functional tool for controlling silicon structure characteristics.

Statements and Declarations

Conflict of interest. There are no conflicts to declare.

Data availability statement. Some or all data generated or used during the study are available from the corresponding author by request.

Funding. This work was supported by National Research Foundation of Ukraine (project number 2020.02/0036).

Author Contributions. All authors contributed equally to this work.

References

- [1] Ostapenko, S.S., Korsunskaya, N.E., Sheinkman, M.K.: Ultrasound stimulated defect reactions in semiconductors. In: Defect Interaction and Clustering in Semiconductors. Solid State Phenomena, vol. 85–86, pp. 317–336. Trans Tech Publications Ltd, Zürich (2002). <https://doi.org/10.4028/www.scientific.net/SSP.85-86.317>
- [2] Savkina, R.K.: Recent progress in semiconductor properties engineering by ultrasonication. Recent Patents on Electrical & Electronic Engineering **6**(3), 157–172 (2013). <https://doi.org/10.2174/22131116113066660008>
- [3] Olikh, O.Y., Gorb, A.M., Chupryna, R.G., Pristay–Fenenkov, O.V.: Acousto–defect interaction in irradiated and non–irradiated silicon $n^+–p$ structure. J. Appl. Phys. **123**(16), 161573 (2018). <https://doi.org/10.1063/1.5001123>
- [4] Davletova, A., Karazhanov, S.Z.: Open-circuit voltage decay transient in dislocation-engineered Si p–n junction. Journal of Physics D: Applied Physics **41**(16), 165107 (2008). <https://doi.org/10.1088/0022-3727/41/16/165107>
- [5] Olikh, Y., Tymochko, M., Olikh, O.: Mechanisms of two-stage conductivity relaxation in cdte:cl with ultrasound. J. Electron. Mater. **49**(8), 4524–453 (2020). <https://doi.org/10.1007/s11664-020-08179-7>
- [6] Olikh, O.: Reversible influence of ultrasound on γ –irradiated Mo/n-Si Schottky barrier structure. Ultrasonics **56**, 545–550 (2015). <https://doi.org/10.1016/j.ultras.2014.10.008>
- [7] Olikh, O.Y., Voytenko, K.V., Burbelo, R.M.: Ultrasound influence on I–V–T characteristics of silicon Schottky barrier structure. J. Appl. Phys. **117**(4), 044505 (2015). <https://doi.org/10.1063/1.4906844>
- [8] Sukach, A.V., Teterkin, V.V.: Ultrasonic treatment–induced modification of the electrical properties of InAs p–n junctions. Tech. Phys. Lett. **35**(6), 514–517 (2009). <https://doi.org/10.1134/S1063785009060108>
- [9] Krüger, D., Romanyuk, B., Melnik, V., Olikh, Y., Kurps, R.: Influence of in situ ultrasound treatment during ion implantation on amorphization and junction formation in silicon. J. Vac. Sci. Technol. B **20**(4), 1448–1451 (2002). <https://doi.org/10.1116/1.1493784>
- [10] Romanyuk, B., Melnik, V., Olikh, Y., Popov, V., Krüger, D.: Modification of the si amorphization process by in situ ultrasonic treatment during ion implantation. Semicond. Sci. Technol. **16**(5), 397–401 (2001). <https://doi.org/10.1088/0268-1242/16/5/320>

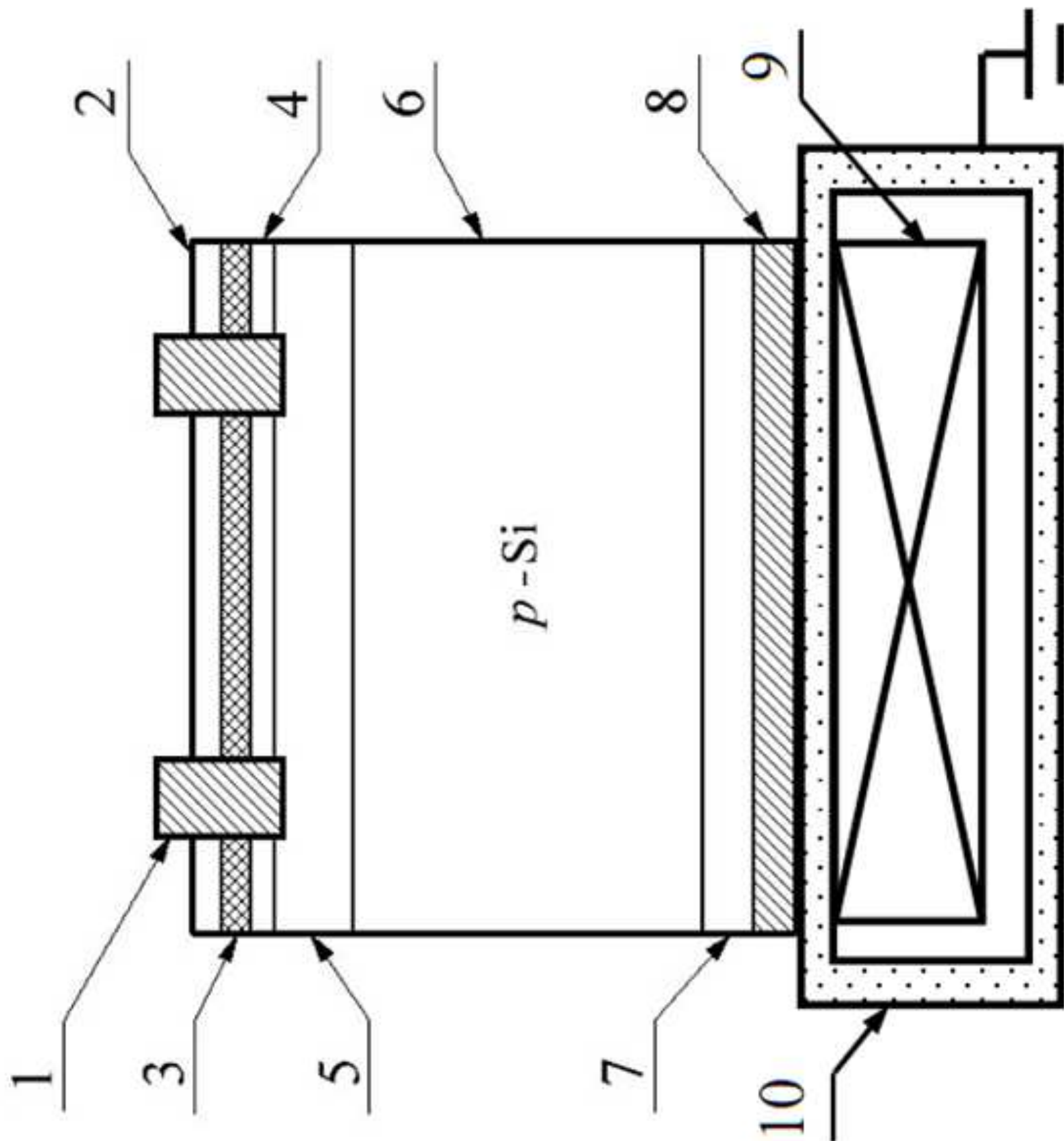
- [11] Kalem, S., Yavuzcetin, O., Altineller, C.: Effect of light exposure and ultrasound on the formation of porous silicon. *Journal of Porous Materials* **7**(1), 381–383 (2000). <https://doi.org/10.1023/A:1009687021287>
- [12] Fujita, S., Kaneko, K., Ikenoue, T., Kawaharamura, T., Furuta, M.: Ultrasonic-assisted mist chemical vapor deposition of ii-oxide and related oxide compounds. *Phys. Status Solidi C* **11**(7–8), 1225–1228 (2014). <https://doi.org/10.1002/pssc.201300655>
- [13] Istratov, A.A., Hieslmair, H., Weber, E.R.: Iron and its complexes in silicon. *Applied Physics A: Materials Science & Processing* **69**(1), 13–44 (1999). <https://doi.org/10.1007/s003390050968>
- [14] Schubert, M.C., Padilla, M., Michl, B., Mundt, L., Giesecke, J., Hohl-Ebinger, J., Benick, J., Warta, W., Tajima, M., Ogura, A.: Iron related solar cell instability: Imaging analysis and impact on cell performance. *Sol. Energy Mater. Sol. Cells* **138**, 96–101 (2015). <https://doi.org/10.1016/j.solmat.2015.03.001>
- [15] Laine, H.S., Vähänissi, V., Morishige, A.E., Hofstetter, J., Haarahiltunen, A., Lai, B., Savin, H., Fenning, D.P.: Impact of iron precipitation on phosphorus-implanted silicon solar cells. *IEEE Journal of Photovoltaics* **6**(5), 1094–1102 (2016). <https://doi.org/10.1109/JPHOTOV.2016.2576680>
- [16] Vähänissi, V., Haarahiltunen, A., Talvitie, H., Yli-Koski, M., Savin, H.: Impact of phosphorus gettering parameters and initial iron level on silicon solar cell properties. *Progress in Photovoltaics: Research and Applications* **21**(5), 1127–1135 (2013). <https://doi.org/10.1002/pip.2215>
- [17] Mchedlidze, T., Möller, C., Lauer, K., Weber, J.: Evolution of iron-containing defects during processing of si solar cells. *J. Appl. Phys.* **116**(24), 245701 (2014). <https://doi.org/10.1063/1.4905027>
- [18] Bartel, T., Gibaja, F., Graf, O., Gross, D., Kaes, M., Heuer, M., Kirscht, F., Möller, C., Lauer, K.: Dynamics of iron-acceptor-pair formation in co-doped silicon. *Appl. Phys. Lett.* **103**(20), 202109 (2013). <https://doi.org/10.1063/1.4830227>
- [19] Ajayan, J., Nirmal, D., Mohankumar, P., Saravanan, M., Jagadesh, M., Arivazhagan, L.: A review of photovoltaic performance of organic/inorganic solar cells for future renewable and sustainable energy technologies. *Superlattices Microstruct.* **143**, 106549 (2020). <https://doi.org/10.1016/j.spmi.2020.106549>
- [20] Green, M.A.: Photovoltaic technology and visions for the future. *Prog. Energy* **1**(1), 013001 (2019). <https://doi.org/10.1088/2516-1083/ab0fa8>

- 14 *Intensification of FeB association in Si-SCs by acoustic wave*
- [21] Ostapenko, S.S., Jastrzebski, L., Lagowski, J., Sopori, B.: Increasing short minority carrier diffusion lengths in solar-grade polycrystalline silicon by ultrasound treatment. *Appl. Phys. Lett.* **65**(12), 1555–1557 (1994). <https://doi.org/10.1063/1.112942>
- [22] Ostapenko, S.S., Bell, R.E.: Ultrasound stimulated dissociation of Fe–B pairs in silicon. *J. Appl. Phys.* **77**(10), 5458–5460 (1995). <https://doi.org/10.1063/1.359243>
- [23] Brailsford, A.D.: Abrupt-kink model of dislocation motion. *Phys. Rev.* **122**(3), 778–786 (1961). <https://doi.org/10.1103/PhysRev.122.778>
- [24] Pavlovich, V.N.: Enhanced diffusion of impurities and defects in crystals in conditions of ultrasonic and radiative excitation of the crystal lattice. *Phys. Status Solidi B* **180**(1), 97–105 (1993). <https://doi.org/10.1002/pssb.2221800108>
- [25] Peleshchak, R.M., Kuzyk, O.V., Dan’kiv, O.O.: Formation of periodic structures under the influence of an acoustic wave in semiconductors with a two-component defect subsystem. *Ukr. J. Phys.* **61**(8), 741–746 (2016). <https://doi.org/10.15407/ujpe61.08.0741>
- [26] Olikh, O.Y.: Acoustically driven degradation in single crystalline silicon solar cell. *Superlattices Microstruct.* **117**, 173–188 (2018). <https://doi.org/10.1016/j.spmi.2018.03.027>
- [27] Wijaranakula, W.: The reaction kinetics of iron–boron pair formation and dissociation in p-type silicon. *J. Electrochem. Soc.* **140**(1), 275–281 (1993). <https://doi.org/10.1149/1.2056102>
- [28] Möller, C., Bartel, T., Gibaja, F., Lauer, K.: Iron-boron pairing kinetics in illuminated p-type and in boron/phosphorus co-doped n-type silicon. *J. Appl. Phys.* **116**(2), 024503 (2014). <https://doi.org/10.1063/1.4889817>
- [29] Tan, J., Macdonald, D., Rougieux, F., Cuevas, A.: Accurate measurement of the formation rate of iron–boron pairs in silicon. *Semicond Sci. Technol.* **26**(5), 055019 (2011). <https://doi.org/10.1088/0268-1242/26/5/055019>
- [30] Macdonald, D., Roth, T., Deenapanray, P.N.K., Bothe, K., Pohl, P., Schmidt, J.: Formation rates of iron-acceptor pairs in crystalline silicon. *J. Appl. Phys.* **98**(8), 083509 (2005). <https://doi.org/10.1063/1.2102071>
- [31] Lindroos, J., Savin, H.: Review of light-induced degradation in crystalline silicon solar cells. *Sol. Energy Mater. Sol. Cells* **147**, 115–126 (2016). <https://doi.org/10.1016/j.solmat.2015.11.047>
- [32] Schmid, A., Fischer, C., Skorka, D., Herguth, A., Winter, C., Zuschlag,

- A., Hahn, G.: On the role of AlO_x thickness in $\text{AlO}_x/\text{SiN}_y$: H layer stacks regarding light- and elevated temperature-induced degradation and hydrogen diffusion in c-Si. *IEEE Journal of Photovoltaics* **11**(4), 967–973 (2021). <https://doi.org/10.1109/JPHOTOV.2021.3075850>
- [33] Wagner, M., Wolny, F., Hentsche, M., Krause, A., Sylla, L., Kropfgans, F., Ernst, M., Zierer, R., Bönisch, P., Müller, P., Schmidt, N., Osinniy, V., Hartmann, H.-P., Mehnert, R., Neuhaus, H.: Correlation of the LeTID amplitude to the Aluminium bulk concentration and Oxygen precipitation in PERC solar cells. *Sol. Energy Mater. Sol. Cells* **187**, 176–188 (2018). <https://doi.org/10.1016/j.solmat.2018.06.009>
- [34] Chen, D., Kim, M., Stefani, B.V., Hallam, B.J., Abbott, M.D., Chan, C.E., Chen, R., Payne, D.N.R., Nampalli, N., Ciesla, A., Fung, T.H., Kim, K., Wenham, S.R.: Evidence of an identical firing-activated carrier-induced defect in monocrystalline and multicrystalline silicon. *Sol. Energy Mater. Sol. Cells* **172**, 293–300 (2017). <https://doi.org/10.1016/j.solmat.2017.08.003>
- [35] Fahrenbruch, A., Bube, R.: *Fundamentals of Solar Cells: Photovoltaic Solar Energy Conversion*, p. 580. Academic Press, NY, London, Paris (1983)
- [36] Razeghi, M., Rogalski, A.: Semiconductor ultraviolet detectors. *J. Appl. Phys.* **79**(10), 7433–7473 (1996). <https://doi.org/10.1063/1.362677>
- [37] Rajkanan, K., Singh, R., Shewchun, J.: Absorption coefficient of silicon for solar cell calculations. *Solid-State Electron.* **22**(9), 793–795 (1979). [https://doi.org/10.1016/0038-1101\(79\)90128-X](https://doi.org/10.1016/0038-1101(79)90128-X)
- [38] Green, M.A., Keevers, M.J.: Optical properties of intrinsic silicon at 300 k. *Progress in Photovoltaics: Research and Applications* **3**(3), 189–192 (1995). <https://doi.org/10.1002/pip.4670030303>
- [39] Klyui, N.I., Kostlyov, V.P., Rozhin, A.G., Gorbulik, V.I., Litovchenko, V.G., Voronkin, M.A., Zaika, N.I.: Silicon solar cells with antireflecting and protective coatings based on diamond-like carbon and silicon carbide films. *Opto-Electr. Rev.* **8**(4), 402–405 (2000)
- [40] Litovchenko, V.G., Klyui, N.I., Kostlyov, V.P., Gorbulik, V.I., Piryatinskii, Y.P.: Nitrogen containing diamond-like carbon films as protective and fluorescent layers for silicon solar cells. *Opto-Electr. Rev.* **8**(4), 406–409 (2000)
- [41] Klaassen, D.B.M.: A unified mobility model for device simulation — I. model equations and concentration dependence. *Solid-State Electron.* **35**(7), 953–959 (1992). [https://doi.org/10.1016/0038-1101\(92\)90325-7](https://doi.org/10.1016/0038-1101(92)90325-7)

- 16 *Intensification of FeB association in Si-SCs by acoustic wave*
- [42] Nguyen, H.T., Baker–Finch, S.C., Macdonald, D.: Temperature dependence of the radiative recombination coefficient in crystalline silicon from spectral photoluminescence. *Appl. Phys. Lett.* **104**(11), 112105 (2014). <https://doi.org/10.1063/1.4869295>
- [43] Altermatt, P.P., Schmidt, J., Heiser, G., Aberle, A.G.: Assessment and parameterisation of Coulomb–enhanced Auger recombination coefficients in lowly injected crystalline silicon. *J. Appl. Phys.* **82**(10), 4938–4944 (1997). <https://doi.org/10.1063/1.366360>
- [44] Couderc, R., Amara, M., Lemiti, M.: Reassessment of the intrinsic carrier density temperature dependence in crystalline silicon. *J. Appl. Phys.* **115**(9), 093705 (2014). <https://doi.org/10.1063/1.4867776>
- [45] Green, M.A.: Intrinsic concentration, effective densities of states, and effective mass in silicon. *J. Appl. Phys.* **67**(6), 2944–2954 (1990). <https://doi.org/10.1063/1.345414>
- [46] Rougieux, F.E., Sun, C., Macdonald, D.: Determining the charge states and capture mechanisms of defects in silicon through accurate recombination analyses: A review. *Sol. Energy Mater. Sol. Cells* **187**, 263–272 (2018). <https://doi.org/10.1016/j.solmat.2018.07.029>
- [47] Murphy, J.D., Bothe, K., Olmo, M., Voronkov, V.V., Falster, R.J.: The effect of oxide precipitates on minority carrier lifetime in p–type silicon. *J. Appl. Phys.* **110**(5), 053713 (2011). <https://doi.org/10.1063/1.3632067>
- [48] Mohamed, A.W., Hadi, A.A., Jambi, K.M.: Novel mutation strategy for enhancing SHADE and LSHADE algorithms for global numerical optimization. *Swarm Evol. Comput.* **50**, 100455 (2019). <https://doi.org/10.1016/j.swevo.2018.10.006>
- [49] Zoth, G., Bergholz, W.: A fast, preperetion-free method to detect iron in silicon. *J. Appl. Phys.* **67**(11), 6764–6771 (1990). <https://doi.org/10.1063/1.345063>
- [50] Macdonald, D., Cuevas, A., Geerligs, L.J.: Measuring dopant concentrations in compensated p–type crystalline silicon via iron–acceptor pairing. *Appl. Phys. Lett.* **92**(20), 202119 (2008). <https://doi.org/10.1063/1.2936840>
- [51] Khelifati, N., Laine, H.S., Vähänissi, V., Savin, H., Bouamama, F.Z., Bouhafs, D.: Dissociation and formation kinetics of iron–boron pairs in silicon after phosphorus implantation gettering. *Phys Status Solidi A* **216**(17), 1900253 (2019). <https://doi.org/10.1002/pssa.201900253>
- [52] Aziz, M.J.: Stress effects on defects and dopant diffusion in Si. *Mater.*

- Sci. Semicond. Process. **4**(5), 397–403 (2001). [https://doi.org/10.1016/S1369-8001\(01\)00014-2](https://doi.org/10.1016/S1369-8001(01)00014-2)
- [53] Stavola, M. (ed.): Identification of Defects in Semiconductors. Academic Press, San Diego, Ca (1998)
- [54] Weber, E.R.: Transition metals in silicon. Appl. Phys. A **30**(1), 1–22 (1983). <https://doi.org/10.1007/BF00617708>
- [55] Ostapenko, S.: Defect passivation using ultrasound treatment: fundamentals and application. Applied Physics A: Materials Science & Processing **69**(2), 225–232 (1999). <https://doi.org/10.1007/s003390050994>
- [56] Zaveryukhin, B.N., Zaveryukhina, N.N., Tursunkulov, O.M.: Variation of the reflection coefficient of semiconductors in a wavelength range from 0.2 to 20 μm under the action of ultrasonic waves. Tech. Phys. Lett. **28**(9), 752–756 (2002). <https://doi.org/10.1134/1.1511774>
- [57] Ziebarth, B., Mrovec, M., Elsässer, C., Gumbsch, P.: Influence of dislocation strain fields on the diffusion of interstitial iron impurities in silicon. Phys. Rev. B **92**, 115309 (2015). <https://doi.org/10.1103/PhysRevB.92.115309>
- [58] Gorb, A.M., Korotchenkov, O.A., Olikh, O.Y., Podolian, A.O., Chupryna, R.G.: Influence of γ -irradiation and ultrasound treatment on current mechanism in au-sio₂-si structure. Solid-State Electron. **165**, 107712 (2020). <https://doi.org/10.1016/j.sse.2019.107712>
- [59] Kropman, D., Seeman, V., Dolgov, S., Medvids, A.: Effect of ultrasonic treatment on the defect structure of the Si–SiO₂ system. Phys. Status Solidi C **13**(10–12), 793–797 (2016). <https://doi.org/10.1002/pssc.201600052>



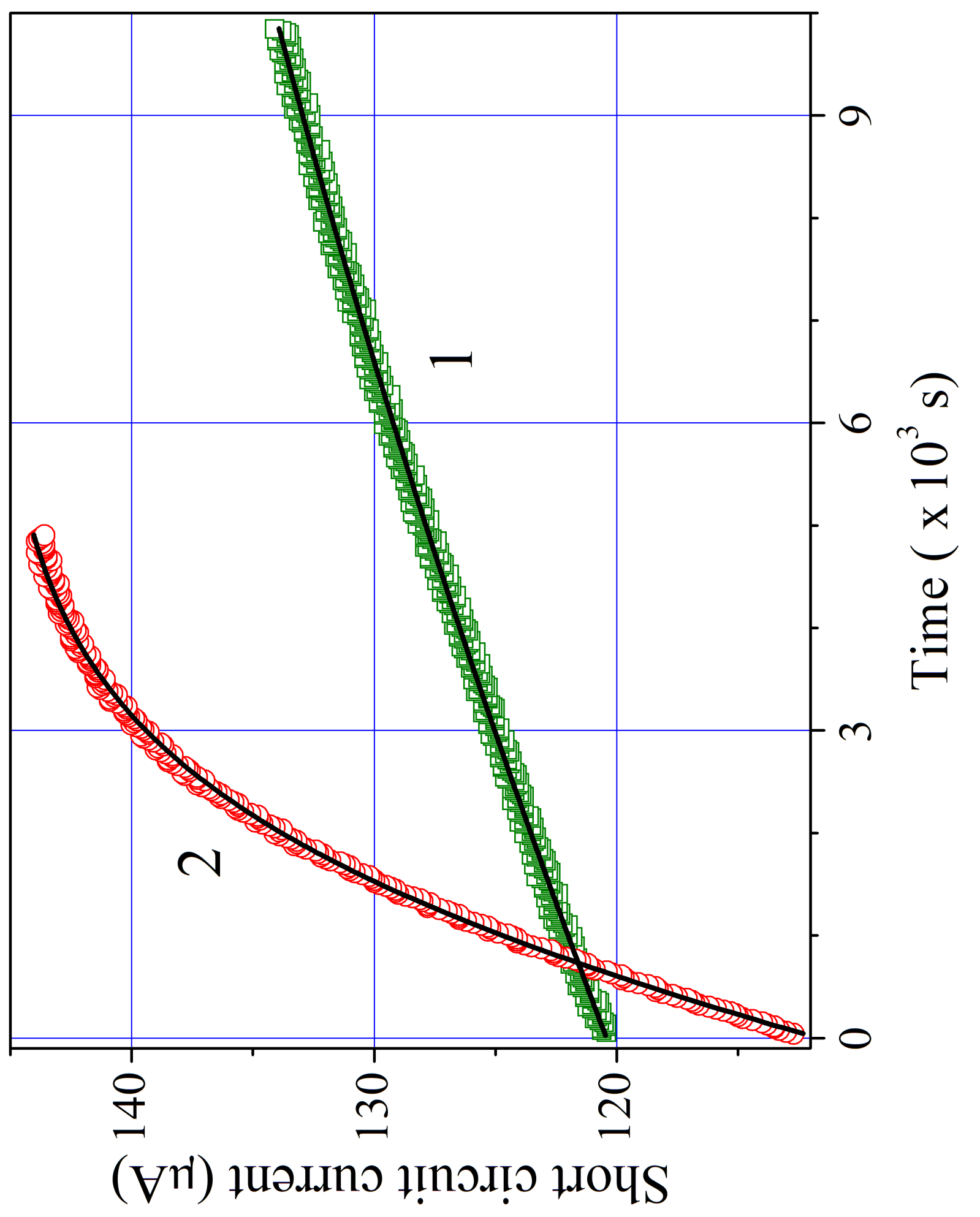
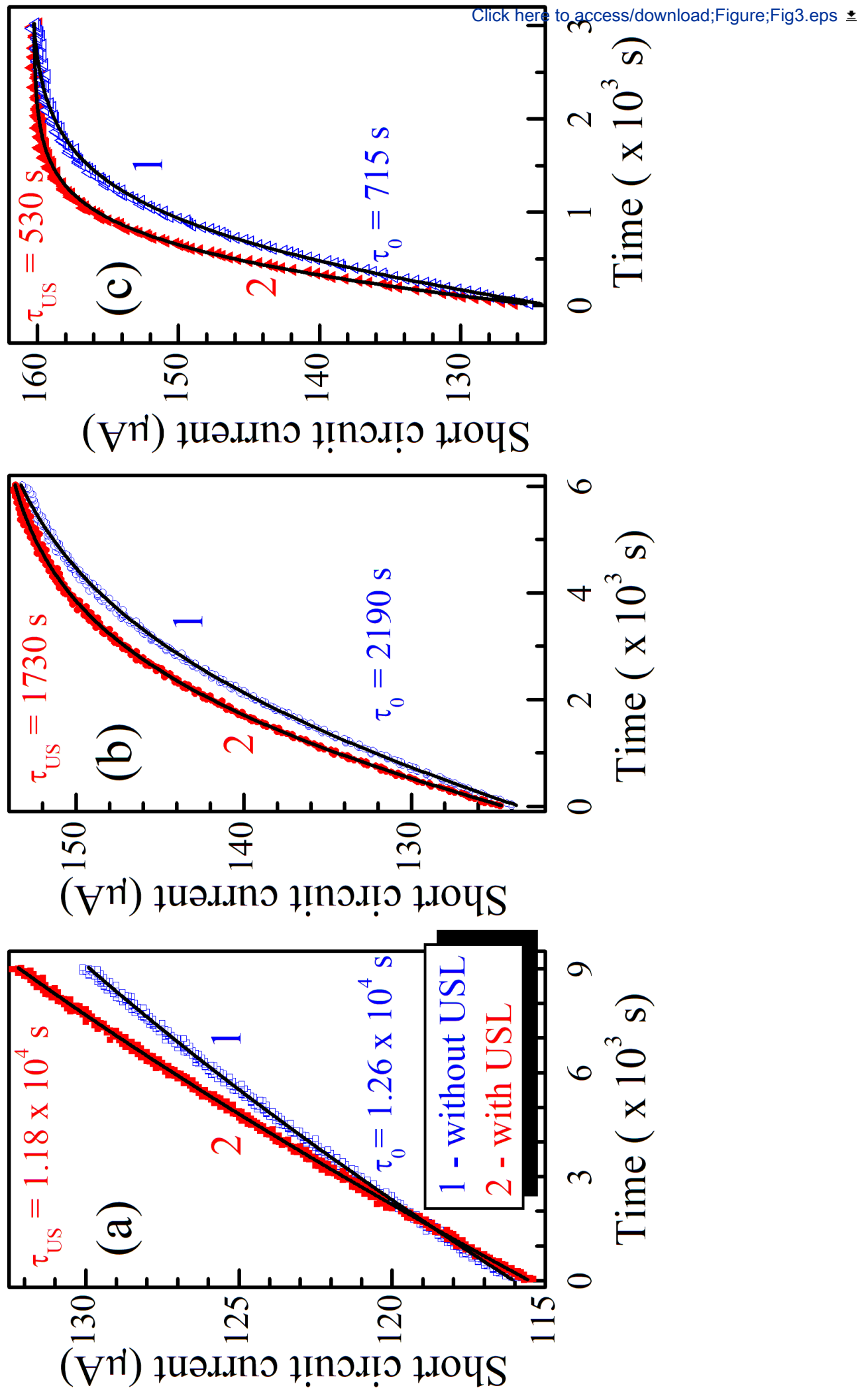
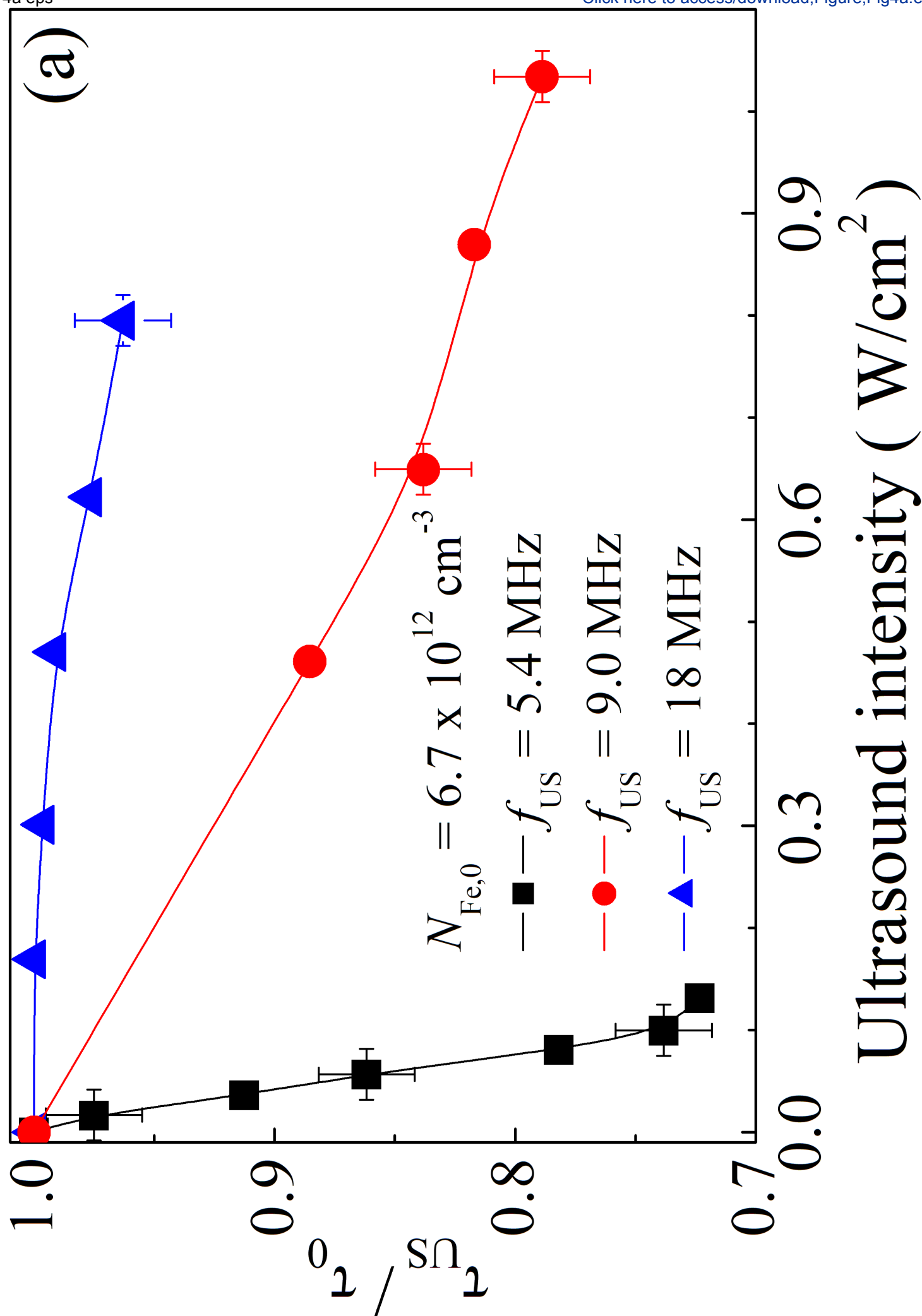


Figure 3 eps





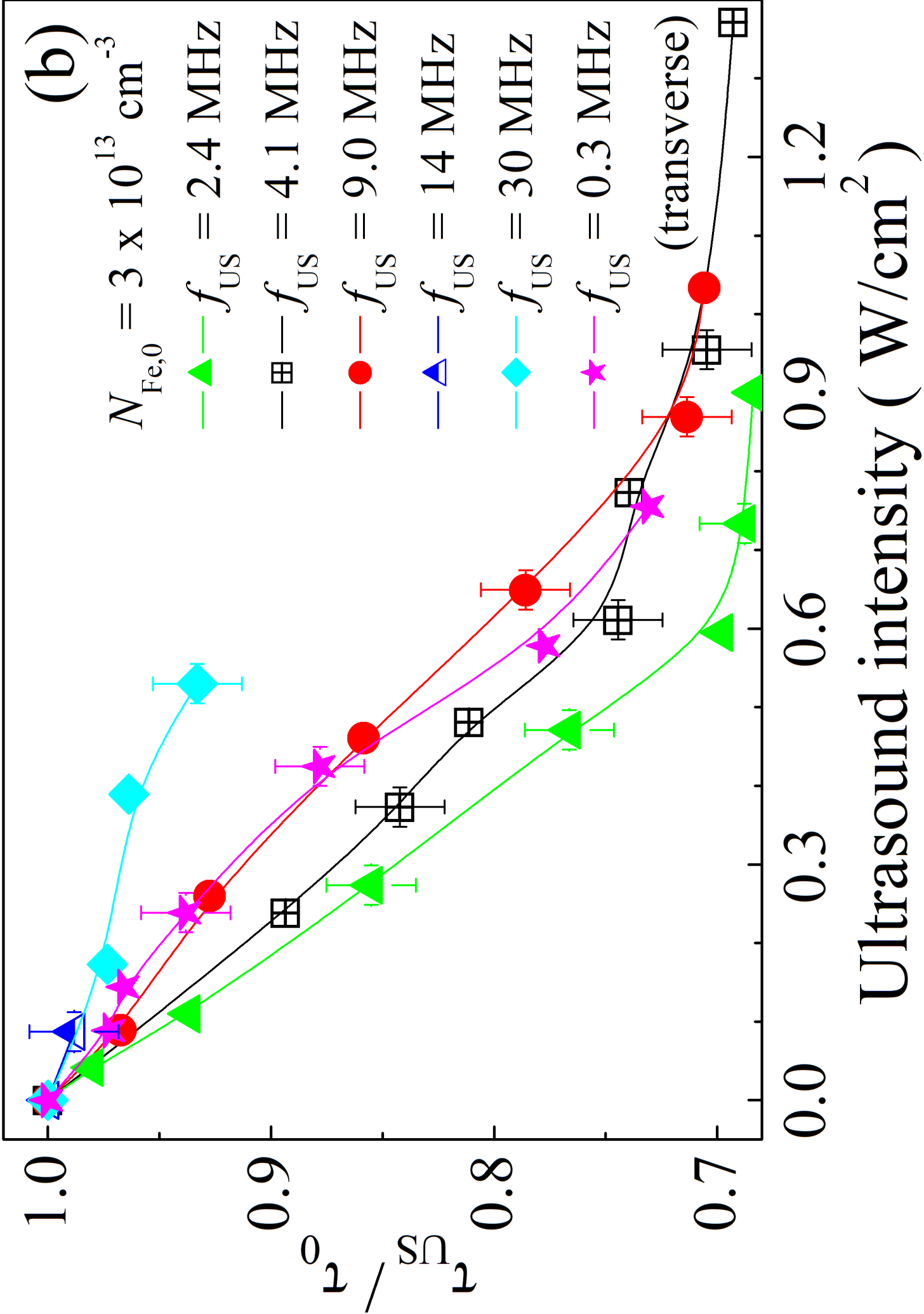
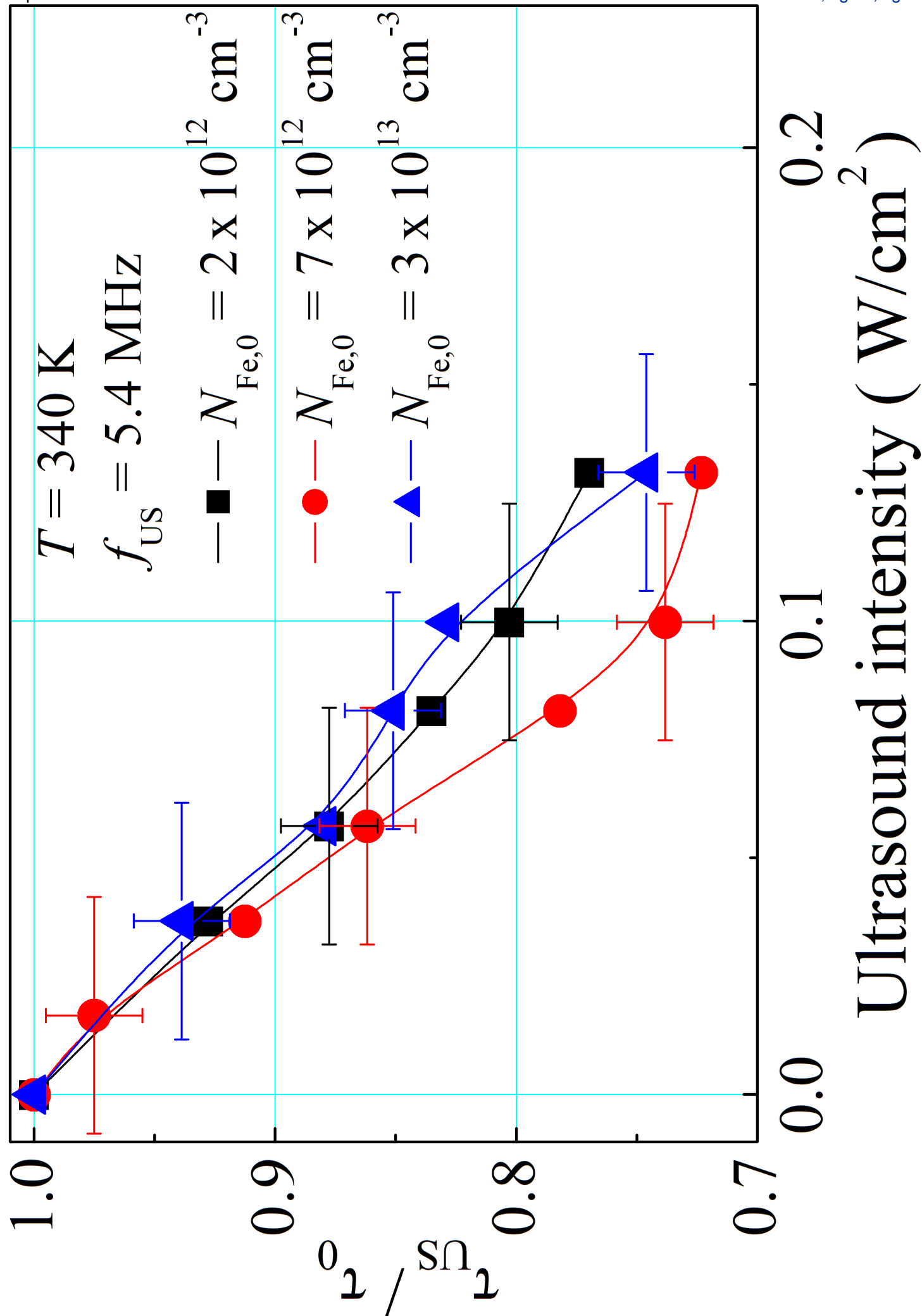
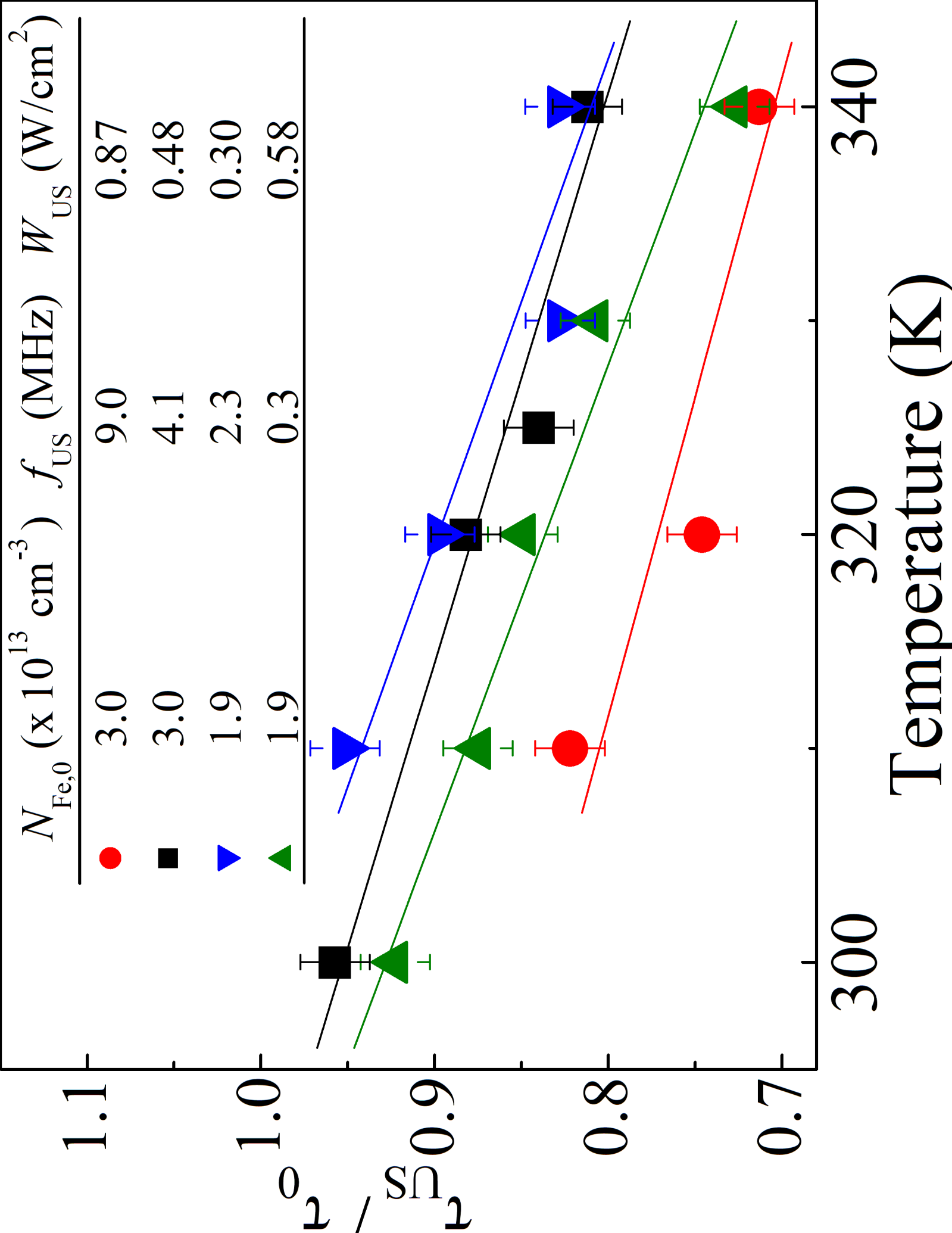
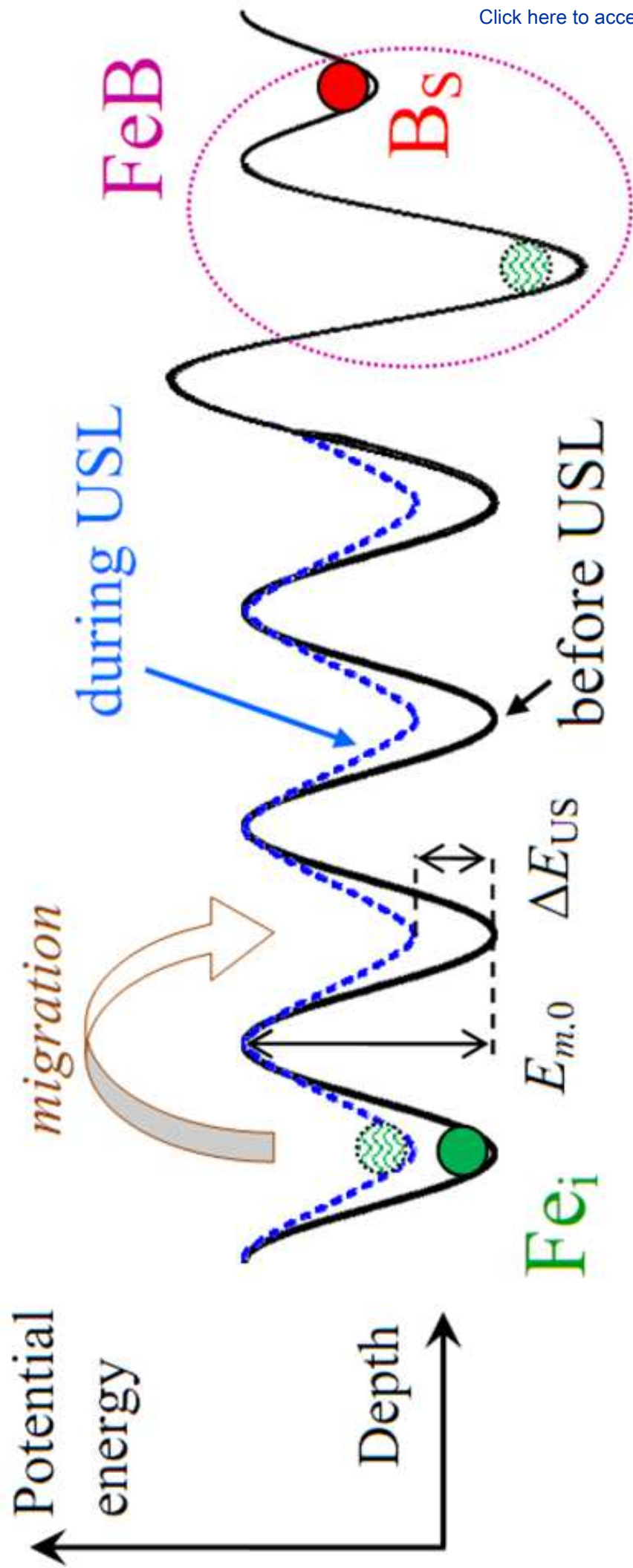
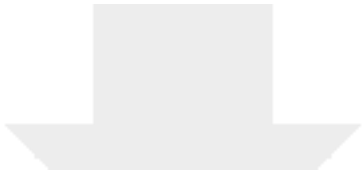


Figure 5 eps

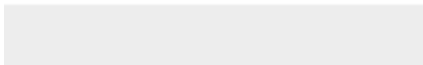



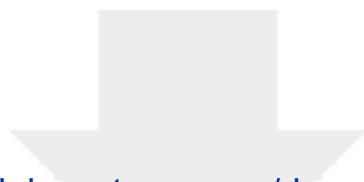






Click here to access/download
Supplementary Material
JMSE_D_22_00483.pdf





[Click here to access/download](#)

Supplementary Material

Marked_JMSE-D-22-00483.pdf

